DOI: 10.1021/ma1017499

Macromolecules
ARTICLE

Influence of Counteranion on the Thermal and Solution Behavior of Poly(2-(dimethylamino)ethyl methacrylate)-Based Polyelectrolytes

Matthew T. Hunley, Jeneffer P. England, and Timothy E. Long*

Macromolecules and Interfaces Institute and Department of Chemistry, Virginia Tech, Blacksburg, Virginia 24061-0212, United States

Received August 1, 2010; Revised Manuscript Received November 3, 2010

ABSTRACT: Poly(2-(dimethylamino)ethyl methacrylate) (PDMAEMA) was synthesized and subsequently neutralized with various acids to form PDMAEMA·HCl, PDMAEMA·HBF_4, and PDMAEMA·HOTf polyelectrolytes. In addition, ion exchange of the chloride anion provided polyelectrolytes with NO_3^-, $N(CN)_2^-$, PF_6^-, and Tf_2N^- anions. The glass transition temperature (T_g) varied significantly with anion in the order $Cl^- > PF_6^- > BF_4^- > NO_3^- > TfO^- > Tf_2N^-$. The polyelectrolytes with larger, weakly coordinated anions required less thermal energy to dissociate ionic interactions, leading to tailored thermal behavior. Solution conductivity of the water-soluble polyelectrolytes decreased in the order $Cl^- > NO_3^- > BF_4^- > N(CN)_2^- > TfO^-$, which was consistent with counteranion mobility. Solution rheology revealed polyelectrolyte behavior for PDMAEMA·HCl, PDMAEMA·HBF_4, and PDMAEMA·HOTf. PDMAEMA·HCl underwent an electrospraying−electrospinning transition at three times the critical concentration for entanglement (C_e), which was consistent with other cationic polyelectrolytes. However, the BF_4^- and TfO^- polyelectrolytes exhibited an onset of fiber formation at $(1.4-1.8)C_e$, much closer to the behavior of neutral, nonassociating polymers. Fiber diameters for all polyelectrolytes were 1−2 orders of magnitude smaller than those for neutral polymers due to increased conductivities of the electrospinning solutions.

Introduction

Ionic liquid monomers provide relatively unexplored families of new charged macromolecules.[1−4] Compared to conventional polyelectrolytes, polymerized ionic liquids typically exhibit lower thermal transitions and enhanced ionic conductivities due to the presence of weakly coordinated ions. The ionic conductivities of these polyelectrolytes approach and often exceed those of polymer films simply doped with conventional ionic liquids. These desirable properties have led to the use of polymerized ionic liquids in many applications including electromechanical actuators,[5,6] photovoltaics,[7] and electrochromic devices.[8]

The physical properties of polymerized ionic liquids depend strongly on the choice of cation and anion. Mercerreyes et al.[9,10] investigated the properties of polycations based on ammonium, imidazolium, and 4-vinylpyridinium cations. They reported that counteranion choice led to significant changes in solubility and thermal stability. The choice of larger, less coordinating anions also led to lower thermal transitions due to increased free volume and weaker ionic interactions. Typically, the larger nonpolar anions (such as $CF_3SO_3^-$ and $(CF_3SO_2)_2N^-$, referred to as TfO^- and Tf_2N^-, respectively) resulted in a significantly increased thermal stability due to the lower basicity and nucleophilicity of the anion. Polyelectrolytes with nonpolar anions also do not dissolve in water but are readily soluble in polar organic solvents. The Elabd research group[2,11] investigated random copolymers incorporating an imidazolium-based ionic liquid acrylic monomer with either BF_4^- or Tf_2N^- counteranions. The ratio of anions was varied to control T_g over the range 265−345 K. The ionic conductivities (at 373 K) of the copolymers in the solid state increased dramatically as the T_g decreased, primarily due to increased mobility of ions in the low-T_g matrix.

*Corresponding author: Tel +1 (540) 231-2480; Fax +1 (540) 231-8517; e-mail telong@vt.edu.

The solution rheological behavior of polyelectrolytes differs significantly from neutral polymers.[12,13] Strong Coulombic repulsion between charged repeat units leads to extended conformations in dilute solution. At higher polymer concentrations, the increased ionic strength reduces the Debye screening length, and the polymer chain contracts to smaller dimensions. Unlike neutral polymers, this contraction leads to a decrease in the chain relaxation time of polyelectrolytes with increasing concentration in semidilute solutions. Specific viscosity (η_{sp}) describes the polymer contribution to viscosity as

$$\eta_{sp} \equiv \frac{\eta_0 - \eta_s}{\eta_s}$$

where η_0 is the zero-shear viscosity of the polymer solution and η_s is the solvent viscosity. In dilute solutions, specific viscosity increases linearly with concentration until the overlap concentration, c^*. Above c^*, in the semidilute unentangled regime, polymer chains begin to experience intermolecular interactions. As concentration increases further, polymer chains become constrained and begin to entangle above the entanglement concentration, c_e. The specific viscosity of polymer solutions scales with concentration in the semidilute unentangled and semidilute entangled regimes as

$$\eta_{sp} \sim C^{1/3\nu - 1} \quad \text{for } C^* < C < C_e$$
$$\eta_{sp} \sim C^{3/3\nu - 1} \quad \text{for } C_e < C < C_D$$

where ν is a geometrical parameter termed the Flory exponent.[13] For neutral polymers in a good solvent, ν equals 0.588, and the scaling exponents for semidilute unentangled and entangled regimes become 1.3 and 3.9, respectively. Polyelectrolytes have elongated conformations in solution and ν equals 1; hence, the scaling exponents are 0.5 and 1.5, respectively. In addition, because of the extended chains in dilute solution, the overlap concentration occurs

 Published on Web 11/17/2010

at lower concentrations and a larger semidilute unentangled regime is observed relative to neutral polymer solutions.

Electrospinning of polymer solutions employs an applied electric field to draw fibers from solution.[14−16] The applied electric potential causes a droplet of solution to form a Taylor cone, and once the applied potential exceeds a critical value, the solution will accelerate toward a grounded or oppositely charged target. The critical voltage occurs as the electrical energy of the Taylor cone exceeds the surface free energy.[17] During flight, the polymer jet experiences significant elongation due to surface charge repulsion; surface tension acts against this repulsion and pulls the jet into droplets. Neutral polymers form electrospun fibers once the solutions become sufficiently elastic to suppress the Rayleigh instability, which leads to breakup of the jet into droplets.[17,18] Our laboratories first demonstrated that neutral, nonassociating polymers exhibit the electrospraying-to-electrospinning transition at concentrations near c_e, and uniform fibers form at higher concentrations near $2c_e$.[18] These transitions corresponded to zero shear viscosities of approximately 10 and 30 cP, respectively. Wilkes and co-workers confirmed this finding and demonstrated that polymers with broad molecular weight distributions require even higher degrees of solution entanglement to form uniform fibers.[19] Wnek and co-workers[17] correlated this transition to the number of entanglements per chain in solution, $(n_e)_{soln}$, and predicted fiber formation at $(n_e)_{soln} = 2$ and uniform fiber formation at $(n_e)_{soln} = 3.5$.

The introduction of surfactants can lower surface tension and aid the formation of bead-free electrospun fibers at lower concentrations.[20,21] In addition, increasing the solution conductivity through introduction of low molar mass electrolytes decreases the concentration required to form uniform fibers.[22,23] The increased conductivity leads to greater stretching of the polymer jet and reduces or eliminates bead formation. A significant reduction in fiber diameter due to this additional stretching also occurs. The addition of small amounts of polyelectrolyte to neutral polymer solutions also facilitates bead suppression in the same manner.[24]

Pure polyelectrolyte solutions present difficulties during electrospinning. Poly(acrylic acid) (PAA) has been successfully electrospun from water and DMF.[25] Uniform fibers were obtained from both solvent systems, although the fibers electrospun from water had larger diameters at similar viscosities and conductivities. However, the fraction of PAA repeat units bearing dissociated carboxylate groups depends on the solution pH and pK_a of the carboxylic acid and is not necessarily 100%. Other polyelectrolytes or ionomers such as poly(allylamine hydrochloride),[26] chitosan,[27] and Nafion[26,28,29] have been successfully electrospun in the presence of neutral polymers. Our research group was the first to electrospin a strong polyelectrolyte, poly(2-(dimethylamino)ethyl methacrylate) hydrogen chloride (PDMAEMA-HCl).[30] The Xia research group[31] electrospun high molecular weight poly(styrenesulfonate) sodium salt at 20 wt % from an 88% formic acid solvent but provided no discussion of solution properties. Recently, Yamamoto et al.[32,33] reported the electrospinning of chitosan from trifluoroacetic acid solution; they thoroughly correlated the electrospinnability to solution viscosity for various molecular weights. Beaded fibers formed above a zero-shear viscosity of 200 cP, and uniform fibers formed above viscosities of 800 cP for several different molecular weight chitosan samples studied. Solutions more viscous than 1000 cP failed to electrospin due to the extremely high viscosity. These solution viscosities are much higher than those observed by Long et al. for neutral nonassociating polymers (beaded fibers above 10 cP, uniform fibers above 30 cP), but an explanation for this discrepancy was not reported, but chitosan will protonate under these acidic conditions, forming a polyelectrolyte. The electrospinning behavior showed marked similarities to that of strong polyelectrolytes. Other polysaccharides exhibited similar difficulties during electrospinning due to their rigid structure and high degree of intermolecular interactions.[34] Yamamoto et al.[35] investigated the electrospinning of cellulose from TFA. The cellulose required extremely high viscosities before uniform fibers collected. Han et al.[36] investigated aqueous solutions of sodium alginate and found that glycerol successfully disrupted the intramolecular hydrogen bonding. The alginate electrospun from glycerol/water solvent systems but still required solution viscosities in excess of 100 000 cP.

Our research group recently reported the rheological characterization and successful electrospinning of the cationic polyelectrolyte PDMAEMA·HCl.[30] Fiber formation required surprisingly high solution concentrations above $8c_e$ and solution viscosities greater than 1000 cP. We hypothesized that the large repulsive forces on the polyelectrolyte chain under an electric field coupled with the relatively low mobility of the polyions led to breakup of the electrospinning jet until sufficient elasticity was present to stabilize the jet. The addition of sodium chloride screened the charges on the polyelectrolyte chain and resulted in lower entanglement numbers and viscosities required for electrospinning.

In the present study, we have synthesized a series of polyelectrolytes based on PDMAEMA, with counteranions of Cl^-, BF_4^-, NO_3^-, $N(CN)_2^-$, PF_6^-, TfO^-, and Tf_2N^-. Thermal degradation temperatures increased 100 °C, and the glass transition temperature decreased 130 °C through simple anion exchange. The choice of counteranion also had a significant effect on solution conductivity and electrospinning behavior. We analyzed the electrospinning behavior in terms of previously developed semiempirical correlations for neutral polymers and observations for polyelectrolytes. PDMAEMA·HCl exhibited typical polyelectrolyte electrospinning behavior, but as the anion was exchanged to BF_4^- and TfO^-, electrospinning behavior resembled neutral polymers in the presence of salt.

Experimental Section

Materials. The monomer 2-(*N*,*N*-dimethylamino)ethyl methacrylate (DMAEMA) (98%) was purchased from Sigma-Aldrich and passed through a silica column to remove inhibitor prior to use. 2,2′-Azobis(isobutyronitrile) (AIBN) (Sigma-Aldrich, 98%) was recrystallized from methanol. Sodium dicyanamide (Sigma-Aldrich, 96%), sodium nitrate (Sigma-Aldrich, 98%), trifluoromethanesulfonic acid (Sigma-Aldrich, 98%), potassium hexafluorophosphate (Sigma-Aldrich, 98%), lithium bis(trifluoromethane)sulfonimide (Fluka, puriss.), and tetrafluoroboric acid (Sigma-Aldrich, 48 wt % solution in water) were used without further purification. Tetrahydrofuran (THF), hexanes, methanol, hydrochloric acid, and deionized water were obtained from commercial sources and used as received.

Polymerization of DMAEMA. In a sample polymerization, 35.7 mL of DMAEMA (33.3 g, 0.211 mol, 20 wt %) was added to 150 mL of THF in a two-necked, round-bottomed flask equipped with a magnetic stir bar. The flask was attached to a reflux condenser and submerged into an oil bath at 65 °C. After the flask was purged with N_2 for 10 min, 0.0346 g of AIBN (0.211 mmol, 0.1 mol % versus DMAEMA) was added, and the reaction mixture was purged with N_2 for another 10 min. The polymerization proceeded at 65 °C for 24 h. After 24 h, the reaction mixture was concentrated and precipitated into 4 L of hexanes and stirred for 2 h. The solvent was decanted, and the polymer dried *in vacuo* overnight at 65 °C. The typical yield after isolation was 60−70%. ^{1}H NMR (400 MHz, $CDCl_3$, δ): 4.1−3.9 (s, 2H, $-OCHH_2-$), 2.6−2.5 (s, 2H $-CH_2N-$), 2.3−2.2 (s, 6H, $-NCH_3$), 2.0−1.7 (s, 2H, $-CH_2-$), 1.1−0.8 (s, 3H, $-CH_3$).

Protonation and Anion Exchange of PDMAEMA. PDMAEMA was dissolved at 10 wt % in deionized water and subsequently titrated with HCl, HBF_4, or CF_3SO_3H to pH 5 to form PDMAEMA·HCl, PDMAEMA·HBF_4, or PDMAEMA·HOTf, respectively. After stirring for 8 h, the polyelectrolyte solution was precipitated into acetone, decanted, and dried *in vacuo* overnight at 65 °C. ^{1}H NMR (400 MHz, D_2O, δ): 11.7−11.4 (s, 1H, NH),

Scheme 1. Synthesis of PDMAEMA and Neutralization with Acid To Form the Polyelectrolytes PDMAEMA·HCl, PDMAEMA·HBF_4, and PDMAEMA·HOTf

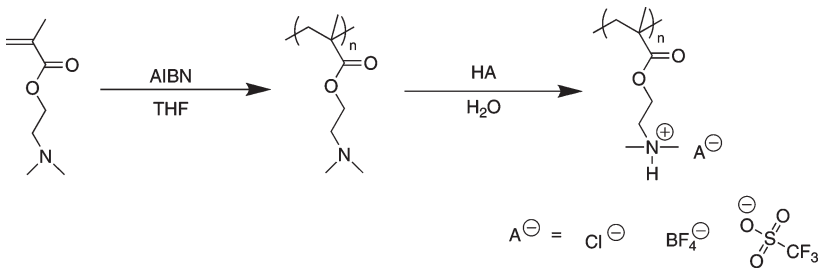

4.5−4.2 (s, 2H, $-OCHH_2-$), 3.6−3.3 (s, 2H, $-CH_2N$), 3.0−2.7 (s, 6H, $-NCH_3$), 2.2−1.8 (s, 2H, $-CH_2-$), 1.2−0.7 (s, 3H, $-CH_3$).

Anion exchanges of PDMAEMA·HCl were performed by either precipitation or dialysis. In a typical precipitation anion exchange, 0.324 g of PDMAEMA·HCl (1.7 mmol of repeat unit) was dissolved in 5 mL of deionized water. Aqueous $Li(CF_3SO_2)_2N$ (2.40 g (8.4 mmol, 5 equiv) in 5 mL of deionized water) was slowly added dropwise to the polymer solution. A white precipitate quickly formed. The precipitate was stirred for 24 h, decanted, and washed thoroughly with deionized water to remove all residual salt. PDMAEMA·HPF_6 was prepared in a similar manner. In a typical dialysis anion exchange, 0.375 g of PDMAEMA·HCl (1.9 mmol of repeat unit) was dissolved in 5 mL of deionized water and added to a solution of 0.863 g of $NaN(CN)_2$ (9.7 mmol, 5 equiv) in 5 mL of deionized water. The mixed solution was syringed into a SpectraPore dialysis cassette (molecular weight cutoff of 3500 g/mol), and the cassette was placed in a beaker of deionized water. After 6 and 12 h, the deionized water was changed and another 0.863 g of $NaN(CN)_2$ added. After another 10 h, the deionized water was changed without salt. This water was changed after an additional 6 and 12 h. Then, the polymer solution was removed from the dialysis cassette and water removed *in vacuo* to isolate the polymer PDMAEMA·$HN(CN)_2$. PDMAEMA·HNO_3 was prepared in a similar manner. XPS analysis confirmed less than 0.2% chlorine in each anion-exchanged polymer.

Analytical Methods. ^{1}H NMR spectra were obtained on a Varian INOVA 400 MHz spectrometer at 23 °C in $CDCl_3$, D_2O, or DMSO-d_6. Thermal analysis was performed on a TA Instruments Q500 thermogravimetric analyzer (TGA) and a TA Instruments Q1000 differential scanning calorimeter (DSC). TGA was conducted from ambient to 600 at 10 °C/min, and DSC was conducted from 0 to 200 at 10 °C/min, using only the second heating scan for analysis. X-ray photoelectron spectroscopy was conducted on a Perkin-Elmer 5300 with a Mg anode at 13 kV accelerating voltage. Size exclusion chromatography was performed as reported previously.[37] Solution conductivity was measured using an ACORN CON6 probe at 25 °C. The average of three measurements was taken. Field emission scanning electron microscopy (FESEM) of electrospun fibers was performed using a LEO 1550 FESEM at 5 keV accelerating voltage. Prior to FESEM analysis, fibers were sputter-coated with 10 nm of 60/40 gold/platinum to prevent excessive charge buildup in the SEM.

Solution Rheology and Electrospinning. Solutions for rheology and electrospinning were prepared by dissolving the desired amount of polymer in an 80/20 (w/w) mixture of deionized water/methanol. The solutions were allowed to stir magnetically for 3 days to ensure equilibration. Solution rheology was conducted on a TA Instruments AR-G2 strain-controlled rheometer equipped with concentric cylinder geometry. The solutions were allowed to equilibrate at 25 °C for 2 min prior to measurement. Solutions for electrospinning were loaded into a syringe equipped with an 18-gauge needle. The syringe was placed into a syringe pump, and the needle was connected to a high-voltage power supply. The polymer solution was metered at a rate of 3 mL/h, and the potential set to 25 kV. Fibers were collected on a grounded, stainless steel mesh target immediately after the voltage was applied. A 1/4 in. × 1/4 in. section of the target was collected for FESEM analysis. Fiber diameters are reported as an average of at least 20 individual measurements along with the standard deviation.

Table 1. SEC Molecular Weights and Thermal Properties of PDMAEMA-Based Polyelectrolytes

polymer	M_n (g/mol)[a]	M_w/M_n[a]	T_g (°C)[b]	$T_{d,5\%}$ (°C)[c]
PDMAEMA	113 000	1.21	19	295
PDMAEMA·HCl (THF)	96 200	1.15	164	230
PDMAEMA·HCl (H_2O)	184 000	1.51	160	230
PDMAEMA·HBF_4	191 000	1.21	131	286
PDMAEMA·HNO_3	96 200	1.15	130	243
PDMAEMA·$HN(CN)_2$	96 200	1.15	n.d.[d]	244
PDMAEMA·HPF_6	96 200	1.15	164	242
PDMAEMA·HOTf	82 200	1.01	70	310
PDMAEMA·$HNTf_2$	96 200	1.15	38	320

[a] Molecular weights and distributions determined by SEC for polymers dialyzed against SEC solvent. [b] Glass transition temperatures measured by DSC. [c] Temperature at 5% weight loss as determined by TGA. [d] No glass transition observed by DSC.

Results and Discussion

Synthesis and Ion Exchange. PDMAEMA was synthesized using conventional free radical polymerization in THF with 0.1 mol % AIBN as initiator. After isolation, the polymer was dissolved in deionized water and titrated with either HCl, HBF_4, or CF_3SO_3H to form the corresponding polyelectrolytes, as illustrated in Scheme 1. XPS analysis confirmed quantitative formation of the polyelectrolytes. As described in our previous report,[37] an aqueous solvent containing 0.7 M $NaNO_3$, 0.1 M Tris, and 200 ppm of NaN_3 (pH adjusted to 6.0 with acetic acid) dissolved the polyelectrolytes and prevented column interactions for molecular weight analysis using size exclusion chromatography. Dynamic light scattering also confirmed that all polyelectrolytes did not aggregate in the SEC solutions. Table 1 lists the molecular weights of all polymers investigated. Each polymer was dialyzed against the SEC solvent before analysis to ensure the only ions in solution were from the solvent. Thus, as shown in Table 1, one would expect that reported molecular weights are independent of the counteranion and reflect the degree of polymerization, easily comparable for all polymers. Number-average molecular weights ranged from 82 200 to 113 000 g/mol. To investigate the effect of molecular weight on electrospinning, higher molecular weight PDMAEMA·HCl and PDMAEMA·HBF_4 were synthesized in DI H_2O using 0.5 wt % ammonium persulfate as the initiator. These two polyelectrolytes had number-average molecular weights of 184 000 and 191 000 g/mol, respectively.

Molecular weight distributions for polyelectrolytes synthesized in THF were lower than expected for conventional free radical polymerizations. However, PDMAEMA·HCl synthesized in water had M_w/M_n of 1.51, which is expected for free radical polymerizations. A sample of PDMAEMA was polymerized in THF to confirm that the low dispersities of the polymers resulted from isolation procedures and not poor

Scheme 2. Anion Exchange of PDMAEMA·HCl To Form PDMAEMA·HNO_3, PDMAEMA·$HN(CN)_2$, PDMAEMA·HPF_6, and PDMAEMA·$HNTf_2$

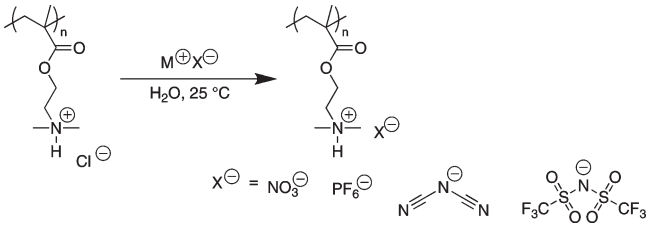

Table 2. Solubility of PDMAEMA-Based Polyelectrolytes in Aqueous and Polar Organic Solvents[a]

polymer	H_2O	0.1 M [NaX][b]	acetone	DMSO
PDMAEMA	+	−	+	+
PDMAEMA·HCl	+	+	−	+
PDMAEMA·HBF_4	+	−	−	+
PDMAEMA·HNO_3	+	+	−	+
PDMAEMA·$HN(CN)_2$	+	+	−	+
PDMAEMA·HPF_6	−	−	+	+
PDMAEMA·HOTf	+	−	+	+
PDMAEMA·$HNTf_2$	−	−	+	+

[a] Solubility indicated by "+" for soluble and "−" for insoluble or only sparingly soluble. [b] [NaX] represents the sodium (or lithium) salt bearing the same anion as the polyelectrolyte. For example, NaCl for PDMAEMA·HCl or $NaBF_4$ for PDMAEMA·HBF_4. NaCl was used for PDMAEMA.

chromatography during SEC analysis. Half of the sample was precipitated in hexanes, consistent with the other polymerizations. The second half of the sample was dialyzed against water and subsequently freeze-dried to remove residual monomer. SEC analysis indicated that the precipitated polymer had M_n = 138 000 g/mol with M_w/M_n = 1.08, and the dialyzed polymer had M_n = 81 100 g/mol with M_w/M_n = 1.30. The precipitation removed much of the lower molecular weight fraction, resulting in an M_n 70% higher and a significantly narrower polydispersity. This analysis confirmed that fractionation during precipitation led to narrow molecular weight distributions observed during SEC analysis.

Anion exchange of the Cl^- anion yielded four new polyelectrolytes with the anions NO_3^-, $N(CN)_2^-$, PF_6^-, and Tf_2N^-, as illustrated in Scheme 2. XPS analysis after anion exchange confirmed complete disappearance of chlorine from all samples. Because these four new polyelectrolytes were prepared from the same PDMAEMA·HCl precursor, the degree of polymerization matched the precursor, and SEC indicated nearly identical molecular weights. All polymers except PDMAEMA·HPF_6 and PDMAEMA·$HNTf_2$ dissolved in water, but only PDMAEMA·HCl, PDMAEMA·HNO_3, and PDMAMA·$HN(CN)_2$ dissolved in 0.1 M salt solutions. DMSO dissolved all polyelectrolytes regardless of counteranion. Table 2 presents the solubilities of each polyelectrolyte in several common polar solvents to form visually clear solutions.

The change of counteranion also affected the resonances of specific protons in the ^1H NMR spectra, most notably the ammonium proton. In DMSO-d_6, this proton appeared at 11.4 ppm for PDMAEMA·HCl but shifted upfield to 10.0 ppm for PDMAEMA·HNO_3, 9.6 ppm for PDMAEMA·HPF_6, and 9.5 ppm for PDMAEMA·HOTf and PDMAEMA·$HNTf_2$. Similar trends, though smaller in magnitude, were observed for the methyl and methylene protons near the ammonium. Shifts in ^1H NMR resonances in imidazolium salts upon ion exchange correlate to the interactions between cation and anion.[38,39] Lungwitz et al.[39] determined the Kamlet−Taft hydrogen-bonding ability of a series of anions with 1-butyl-3-methylimidazolium. They observed a linear relationship between the chemical shift of the proton attached to the 2-position of the imidazolium ring and the hydrogen-bond basicity (β) and acidity (α) of the anion. The upfield shift in the ammonium proton observed in this study also correlated with the α- and β-values for the different anions determined by Lungwitz et al.

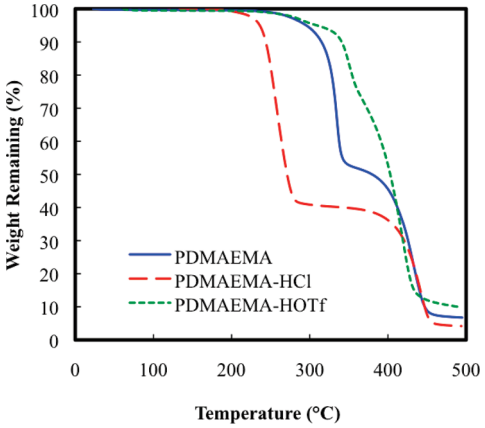

Figure 1. Thermogravimetric analysis of PDMAEMA (solid blue line), PDMAEMA·HCl (dashed red line), and PDMAEMA·HOTf (dotted green line).

Thermal Analysis of PDMAEMA Polyelectrolytes. Thermogravimetric analysis (TGA) indicated the counteranion dictates thermal degradation behavior. Figure 1 shows the TGA thermograms for PDMAEMA and two polyelectrolytes. Neutral PDMAEMA lost ~50% of the initial sample mass at 300 °C and the remainder at 400 °C. For PDMAEMA·HCl, degradation began slightly above 230 °C, with ~60% weight loss occurring in the first step. The remainder of the mass degraded completely around 400 °C. The initial weight loss corresponded to the loss of the anion and ammonium group through the Hofmann elimination mechanism. The second weight loss step involves further degradation of the polymer backbone. The Hofmann elimination reaction depends strongly on the basicity of the anion,[40] and polyelectrolytes with less basic counteranions (such as PDMAEMA·HOTf) did not begin degrading until greater than 300 °C. The onset of degradation is tabulated in Table 1 for all polyelectrolytes.

Anion choice also significantly impacted the polyelectrolyte T_g. Neutral PDMAEMA exhibited a glass transition at 19 °C. The polyelectrolyte PDMAEMA·HCl, however, had a T_g of 164 °C due to the introduction of ionic aggregation. Upon anion exchange to the larger anions, weaker interactions between cation and anion led to reductions in T_g. Polyelectrolyte T_g decreased according to the series $Cl^- > PF_6^- > BF_4^- > NO_3^- > TfO^- > Tf_2N^-$. PDMAEMA·$HPF_6$ exhibited a relatively high T_g of 164 °C, which was presumably due to hydrogen-bonding interactions between the anion and cation. All thermal transitions are listed in Table 1 with the onset of thermal degradation.

Solution Conductivity. Solution conductivity of the water-soluble polyelectrolytes exhibited a strong dependence on the counterion. In aqueous solution, the Cl^- anion dissociated to a large degree from the polymer and led to a high conductivity. The solution conductivity of the polyelectrolytes at constant molar concentration decreased in the order of counterions $Cl^- > NO_3^- > BF_4^- > N(CN)_2^- > TfO^-$, as tabulated in Table 3. The decrease in solution conductivity correlated closely to a decrease in the ionic mobility of the counteranions, as reported in the literature.[41,42] Counterion mobility dominated the conductivity in dilute solutions due to the relatively low mobility of the large polycation.

Table 3. Solution Conductivity of PDMAEMA-Based Polyelectrolytes

anion	conductivity (10^6 S cm^{-1})[a]	ionic mobility (10^{-8} m^2 s^{-1} V^{-1})
[Cl^-]	1705 ± 18	7.91[b]
[NO_3^-]	1670 ± 16	7.40[b]
[BF_4^-]	1559 ± 8	7.77[c]
[$N(CN)_2^-$]	1322 ± 2	5.07[c]
[TfO^-]	1216 ± 7	3.80[c]

[a] Solution conductivity measured in DI H_2O at 298 K at a polymer concentration of 0.15 mol repeat unit/L. [b] At 298 K, from ref 41. [c] At 303 K, estimated from ref 42 using $u = \Lambda/zF$.

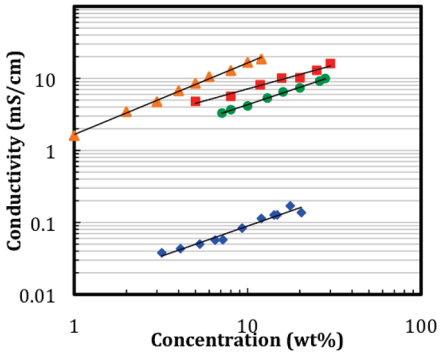

Figure 2. Solution conductivity versus polyelectrolyte concentration for PDMAEMA (diamonds), PDMAEMA·HCl (184 kDa) (triangles), PDMAEMA·HBF_4 (squares), and PDMAEMA·HOTf (circles) in 80/20 H_2O/methanol. The solid lines are power-law fits to the data.

As expected, polymer concentration also had a large effect on the conductivity of the polyelectrolytes, as shown in Figure 2 for PDMAEMA, PDMAEMA·HCl, PDMAEMA·HBF_4, and PDMAEMA·HOTf. These conductivity measurements were performed with a cosolvent of 80/20 (w/w) H_2O/methanol, the same solvent used for subsequent electrospinning. PDMAEMA conductivities ranged from 35 to 175 μS/cm at the selected concentrations, and the data fit a power law relationship with an exponent of 0.84. The polyelectrolytes had conductivities 2 orders of magnitude greater than the neutral polyelectrolyte. The conductivities increased with each counteranion in the same order observed previously in Table 3. Again, the conductivity of each polyelectrolyte fit a power-law relationship, as observed in previous reports for polyelectrolyte solutions in the semidilute regimes.[43,44]

Solution Rheology. Steady-shear rheological experiments were performed on the polyelectrolyte solutions over the semidilute unentangled and entangled regimes. Figure 3 shows the specific viscosity versus concentration for PDMAEMA and the Cl^-, BF_4^-, and TfO^- polyelectrolytes. As expected, viscosity scaling relationships indicated that PDMAEMA behaved as a neutral polymer in water, with scaling factors of 1.2 and 4.4 in the semidilute unentangled and entangled regimes, respectively. The critical concentration for entanglements occurred near 10 wt % based on the transition between these two regimes. The polyelectrolytes exhibited weaker viscosity scaling relationships; the scaling factors above and below entanglement and the estimated c_e values are tabulated in Table 4. The large differences in entanglement concentration resulted from the differences in polyelectrolyte molecular weight. However, the viscosity scaling relationships confirmed that PDMAEMA·HCl, PDMAEMA·HBF_4, and PDMAEMA·HOTf all behaved as strong polyelectrolytes in solution.

Electrospinning. Neutral PDMAEMA and the Cl^-, BF_4^-, and TfO^- polyelectrolytes were electrospun from solutions in the semidilute unentangled and semidilute entangled

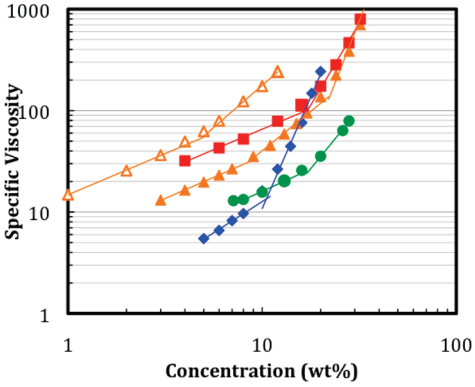

Figure 3. Concentration dependence of specific viscosity for PDMAEMA-based polyelectrolytes in 80/20 H_2O/methanol: PDMAEMA (diamonds), PDMAEMA·HCl (96 kDa) (filled triangles), PDMAEMA·HCl (184 kDa) (open triangles), PDMAEMA·HBF_4 (squares), and PDMAEMA·HOTf (circles). The break in the power-law lines represents the c_e of each polymer.

Table 4. Rheological Scaling Relationships for PDMAEMA Polymers

anion	c_e (wt %)	scaling factor $c^* < c < c_e$	scaling factor $c_e < c < c_D$
neutral	10	1.2	4.4
Cl^- (96 kDa)	9	0.8	1.7
Cl^- (184 kDa)	5	0.8	1.7
BF_4^-	11	0.7	1.5
TfO^-	17	0.8	2.3

regimes to investigate the effect of polyelectrolyte structure on both the onset of fiber formation and fiber diameter relationships. All polymers were electrospun at constant conditions (25 kV, 3 mL/h, 20 cm working distance) from an 80/20 (w/w) H_2O/methanol solvent mixture to ensure changes in electrospinning behavior resulted from solution behavior and not processing parameters. Figure 4 shows FESEM images of electrospun PDMAEMA fibers. The neutral polymer fibers formed a uniform mat on the target at concentrations above c_e. Beaded fiber formation first occurred at a concentration of 12.5 wt % ($\sim 1.2c_e$), and uniform fibers formed at 15 wt % and above ($> 1.5c_e$). Significant fiber fusing was observed in the PDMAEMA fibers due to the low glass transition of the uncharged polymer. The fused fibers were more prevalent at lower concentrations (< 20 wt %), as observed in Figure 4. Average fiber diameters at 12.5 wt % PDMAEMA were 285 ± 102 nm. Fiber diameters increased with concentration to 850 ± 179, 1530 ± 338, and 4560 ± 845 nm for 15, 17.5, and 21 wt % PDMAEMA solutions, respectively. These standard deviations are consistent with prior literature. The onset of fiber formation agreed with our previous results for neutral polymers (beaded fiber formation above c_e and at a viscosity of ~10 cP).[18] However, uniform fibers formed at lower concentrations than expected ($1.5c_e$ instead of $2c_e$). This discrepancy in uniform fiber formation was presumed to result from the low T_g of PDMAEMA, resulting in fiber stretching even after solvent evaporation.

Figure 5 shows the FESEM micrographs of electrospun polyelectrolyte nanofibers. The polyelectrolyte fibers also collected as a uniform mat. Both high and low molecular weight PDMAEMA·HCl exhibited an onset of fiber formation just above $3c_e$ and viscosities just above 300 cP. This higher onset of fiber formation was similar to the previous reports on electrospun cationic PDMAEMA·HCl[30] and chitosan,[32,33] where significantly higher entanglements and viscosities were required to stabilize the electrospinning jet compared to neutral polymers (e.g., PEI-*co*-PET).[18]

Table 5 lists the normalized concentrations (c/c_e) and zero-shear viscosities at the onset of electrospinning for PDMAEMA and the electrospun polyelectrolytes. The entanglement number required for fiber formation decreased with anion as $Cl^- > BF_4^- > TfO^-$. The BF_4^- and TfO^- polyelectrolytes also required only 30 cP solution viscosity to form fibers, 1 order of magnitude lower than PDMAEMA·HCl. Previously, the breakup of the electrospinning jet for polyelectrolytes was attributed to the inter- and intramolecular repulsions of the highly charged polymer chain.[30] The results from this study, as well as those of Chen and Elabd,[11] indicated that polycations with large, hydrophobic anions exhibit electrospinning behavior similar to neutral polymers doped with salt.

Figure 6 compares fiber diameter versus normalized concentration relationship of the electrospun polyelectrolytes with our previously developed semiempirical relationship.[18]

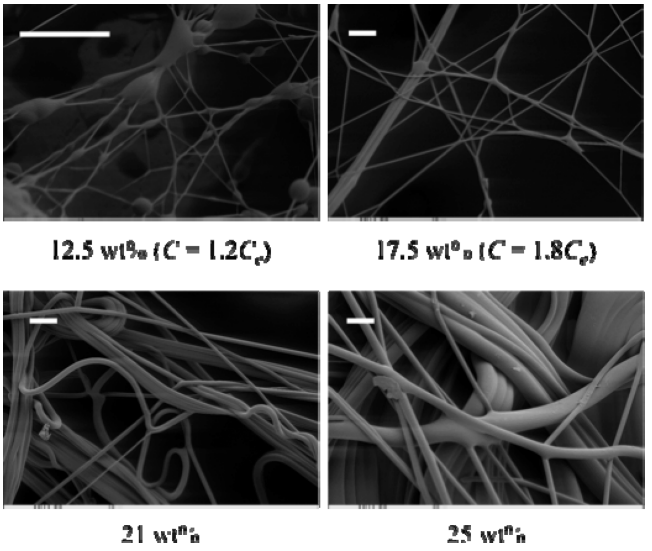

Figure 4. FESEM micrographs depicting electrospun PDMAEMA fibers. The scale bars represent 20 μm.

PDMAEMA exhibited typical electrospinning behavior of a neutral polymer; however, fiber diameters deviated from the nonassociating correlation due to intermolecular associations. The amino group in the PDMAEMA repeat unit exhibited associative interactions, leading to slightly higher fiber diameter scaling relationships. Solution rheology probes these intermolecular associations, and Figure 7 shows the fiber diameter versus zero-shear viscosity. The analysis based on solution flow behavior indicated that PDMAEMA exhibited neutral polymer behavior during electrospinning.

The polyelectrolyte fibers had significantly reduced fiber diameters compared to the neutral polymer fibers (Figure 6). Increased solution conductivity led to increased electrostatic repulsions and stretching of the electrospinning jet, resulting in thinner fibers. Regardless of counteranion, all polyelectrolytes formed fibers with diameters 1−2 orders of magnitude lower than uncharged PDMAEMA due to electrostatic repulsions of the electrospinning jet. Although the counteranion had insignificant effect on the fiber diameters, the more hydrophobic BF_4^- and TfO^- anions decreased the minimum number of entanglements required for stable electrospinning. This also correlated with a reduction in the required zero-shear viscosity at the onset of fiber formation (Figure 7). As discussed earlier, the exchange of Cl^- to the larger BF_4^- and TfO^- anions leads to upfield shifts in ^{1}H NMR resonances of the polyelectrolytes, corresponding with decreasing α- and β-values as well as decreasing polarizability (π^*) of the ion pairs.[35,39,45] Under the large electric

Table 5. Onset of Fiber Formation versus Polymer Counteranion and Molecular Weight

	onset of fiber formation	
anion	c/c_e	η_0 (cP)
neutral	1.2	13
[Cl^-] (96 kDa)	3.1	330
[Cl^-] (184 kDa)	3.2	320
[BF_4^-]	1.8	30
[TfO^-]	1.2	30

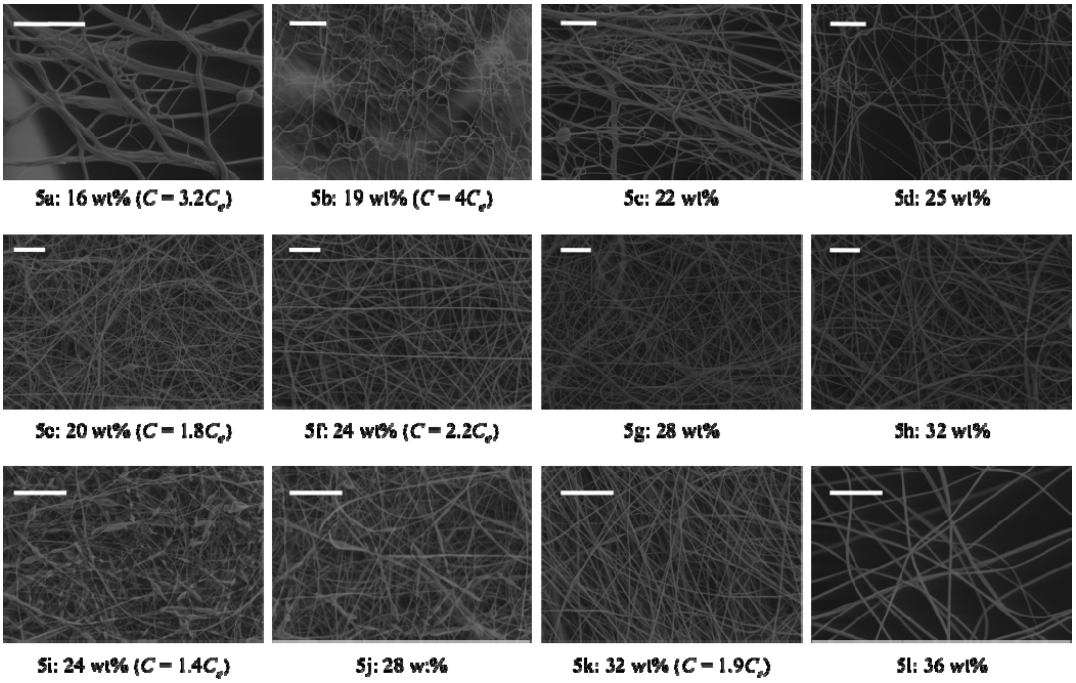

Figure 5. FESEM micrographs depicting electrospun PDMAEMA-based polyelectrolyte fibers: (a−d) PDMAEMA·HCl, (e−h) PDMAEMA·HBF_4, and (i−l) PDMAEMA·HOTf. The scale bars represent 10 μm.

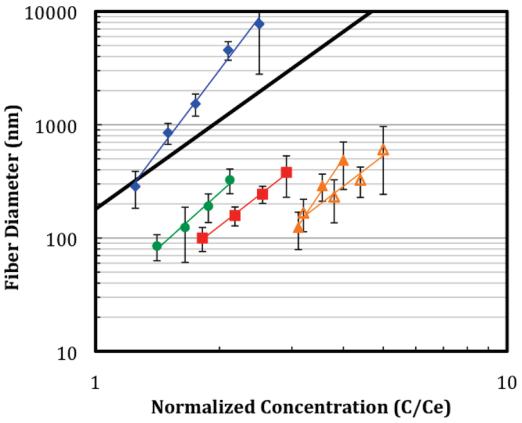

Figure 6. Fiber diameters versus normalized concentration for electrospun PDMAEMA and polyelectrolytes: PDMAEMA (diamonds), PDMAEMA·HCl (96 kDa) (filled triangles), PDMAEMA·HCl (184 kDa) (open triangles), PDMAEMA·HBF_4 (squares), and PDMAEMA·HOTf (circles). The solid line represents a semiempirical correlation for neutral, nonassociating polymers.[18]

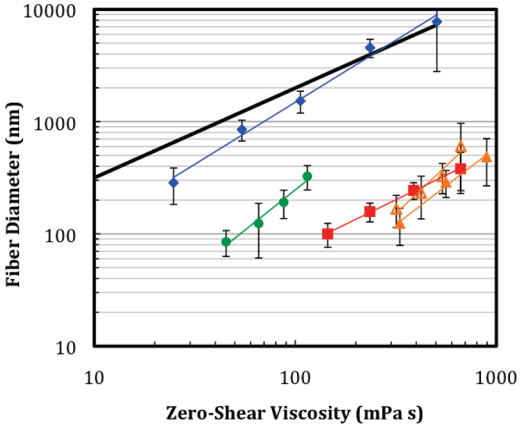

Figure 7. Fiber diameters versus zero shear viscosity for PDMAEMA and polyelectrolytes: PDMAEMA (diamonds), PDMAEMA·HCl (96 kDa) (filled triangles), PDMAEMA·HCl (184 kDa) (open triangles), PDMAEMA·HBF_4 (squares), and PDMAEMA·HOTf (circles). The solid line represents a semiempirical correlation for neutral, nonassociating polymers.[18]

potential during electrospinning, the large polarizability of the Cl^- anion may lead to the instabilities inhibiting electrospinning. However, further experiments are needed to confirm this relationship.

Conclusions

The thermal, solution, and electrospinning properties of a series of polyelectrolytes with varying anions were investigated. Ion exchange from a halide counteranion to larger, ionic-liquid type anions led to significant reductions in glass transition temperature due to weaker ionic interactions. Three polyelectrolytes were investigated in the solution state: PDMAEMA·HCl, PDMAEMA·HBF_4, and PDMAEMA·HOTf. Slight differences in solution conductivity were attributed to differences in counterion mobility, and the rheological behavior of all three polymers indicated polyelectrolyte behavior. For the first time, the electrospinning behavior of polyelectrolytes was correlated with polymer chemical structure. The electrospinning behavior showed significant dependence on counteranion. PDMAEMA·HCl required large entanglement numbers ($>3c_e$) to form fibers, while PDMAEMA·HBF_4 and PDMAEMA·HOTf formed beaded fibers at much lower solution entanglement numbers ($\sim 1-1.5c_e$), similar to neutral polymer behavior. All three polyelectrolytes formed fibers much thinner than predicted for neutral polymers due to the increased ionic conductivity of the electrospinning solutions. The larger, delocalized counteranions enabled fiber formation at lower solution viscosities and solution entanglement numbers, suggesting electrospinning of polyelectrolytes which had previously been difficult to electrospin. This observation allows us to expand the classes of polymers capable of electrospinning to generate high surface area membranes applicable for electromechanical devices.

Acknowledgment. This material is based upon work supported by the U.S. Army Research Laboratory and the U.S. Army Research Office under Contract/Grant W911NF-07-1-0452 Ionic Liquids in Electro-Active Devices Multidisciplinary University Research Initiative (ILEAD MURI).

References and Notes

(1) Green, M. D.; Long, T. E. *Polym. Rev.* **2009**, *49*, 291–314.
(2) Chen, H.; Choi, J.-H.; Salas-de la Cruz, D.; Winey, K. I.; Elabd, Y. A. *Macromolecules* **2009**, *42*, 4809–4816.
(3) Matsumi, N.; Sugai, K.; Miyake, M.; Ohno, H. *Macromolecules* **2006**, *39*, 6924–6927.
(4) Yoshizawa, M.; Ohno, H. *Electrochim. Acta* **2001**, *46*, 1723–1728.
(5) Duncan, A. J.; et al. *Smart Mater. Struct.* **2009**, *18*, 104005.
(6) Duncan, A. J.; Layman, J. M.; Cashion, M. P.; Leo, D. J.; Long, T. E. *Polym. Int.* **2010**, *59*, 25–35.
(7) Taranekar, P.; Qiao, Q.; Jiang, H.; Ghiviriga, I.; Schanze, K. S.; Reynolds, J. R. *J. Am. Chem. Soc.* **2007**, *129*, 8958–8959.
(8) Jain, V.; Khiterer, M.; Montazami, R.; Yochum, H. M.; Shea, K. J.; Heflin, J. R. *ACS Appl. Mater. Interfaces* **2009**, *1*, 83–89.
(9) Marcilla, R.; Blazquez, J. A.; Fernandez, R.; Grande, H.; Pomposo, J. A.; Mecerreyes, D. *Macromol. Chem. Phys.* **2005**, *206*, 299–304.
(10) Marcilla, R.; Blazquez, J. A.; Rodriquez, J.; Pomposo, J. A.; Mecerreyes, D. *J. Polym. Sci., Part A: Polym. Chem.* **2004**, *42*, 208–212.
(11) Chen, H.; Elabd, Y. A. *Macromolecules* **2009**, *42*, 3368–3373.
(12) Dobrynin, A. V.; Rubinstein, M. *Prog. Polym. Sci.* **2005**, *30*, 1049–1118.
(13) Colby, R. H. *Rheol. Acta* **2010**, *49*, 425–442.
(14) Greiner, A.; Wendorff, J. H. *Angew. Chem., Int. Ed.* **2007**, *46*, 5670–5703.
(15) Reneker, D. H.; Yarin, A. L. *Polymer* **2008**, *49*, 2387–2425.
(16) Thavasi, V.; Singh, G.; Ramakrishna, S. *Energy Environ. Sci.* **2008**, *1*, 205–221.
(17) Shenoy, S. L.; Bates, W. D.; Frisch, H. L.; Wnek, G. E. *Polymer* **2005**, *46*, 3372–3384.
(18) McKee, M. G.; Wilkes, G. L.; Colby, R. H.; Long, T. E. *Macromolecules* **2004**, *37*, 1760–1767.
(19) Gupta, P.; Elkins, C.; Long, T. E.; Wilkes, G. L. *Polymer* **2005**, *46*, 4799–4810.
(20) Hunley, M. T.; Harber, A.; Orlicki, J. A.; Rawlett, A. M.; Long, T. E. *Langmuir* **2008**, *24*, 654–657.
(21) Wang, S.-Q.; He, J.-H.; Xu, L. *Polym. Int.* **2008**, *57*, 1079–1082.
(22) Lin, T.; et al. *Nanotechnology* **2004**, *15*, 1375.
(23) Arayanarakul, K.; Choktaweesap, N.; Aht-ong, D.; Meechaisue, C.; Supaphol, P. *Macromol. Mater. Eng.* **2006**, *291*, 581–591.
(24) Jacobs, V.; Anandjiwala, R. D.; Maaza, M. *J. Appl. Polym. Sci.* **2010**, *115*, 3130–3136.
(25) Li, L.; Hsieh, Y.-L. *Polymer* **2005**, *46*, 5133–5139.
(26) Chunder, A.; Sarkar, S.; Yu, Y.; Zhai, L. *Colloids Surf., B* **2007**, *58*, 172–179.
(27) Park, W. H.; Jeong, L.; Yoo, D. I.; Hudson, S. *Polymer* **2004**, *45*, 7151–7157.
(28) Laforgue, A.; Robitaille, L.; Mokrini, A.; Ajji, A. *Macromol. Mater. Eng.* **2007**, *292*, 1229–1236.
(29) Nah, C.; Kwak, S. K.; Kim, N.; Lyu, M.-Y.; Hwang, B. S.; Akle, B.; Leo, D. J. *Key Eng. Mater.* **2007**, *334*−*335*, 1001.
(30) McKee, M. G.; Hunley, M. T.; Layman, J. M.; Long, T. E. *Macromolecules* **2006**, *39*, 575–583.
(31) McCann, J. T.; Lim, B.; Ostermann, R.; Rycenga, M.; Marquez, M.; Xia, Y. *Nano Lett.* **2007**, *7*, 2470–2474.

(32) Ohkawa, K.; Cha, D.; Kim, H.; Nishida, A.; Yamamoto, H. *Macromol. Rapid Commun*. **2004**, *25*, 1600–1605.
(33) Ohkawa, K.; Minato, K.-I.; Kumagai, G.; Hayashi, S.; Yamamoto, H. *Biomacromolecules* **2006**, *7*, 3291–3294.
(34) Lee, K. Y.; Jeong, L.; Kang, Y. O.; Lee, S. J.; Park, W. H. *Adv. Drug Delivery Rev*. **2009**, *61*, 1020–1032.
(35) Ohkawa, K.; Hayashi, S.; Nishida, A.; Yamamoto, H.; Ducreux, J. *Textile Res. J*. **2009**, *79*, 1396–1401.
(36) Nie, H.; He, A.; Zheng, J.; Xu, S.; Li, J.; Han, C. C. *Biomacromolecules* **2008**, *9*, 1362–1365.
(37) Layman, J. M.; Ramirez, S. M.; Green, M. D.; Long, T. E. *Biomacromolecules* **2009**, *10*, 1244–1252.
(38) Lin, S.-T.; Ding, M.-F.; Chang, C.-W.; Lue, S.-S. *Tetrahedron* **2004**, *60*, 9441–9446.
(39) Lungwitz, R.; Friedrich, M.; Linert, W.; Spange, S. *New J. Chem*. **2008**, *32*, 1493–1499.
(40) March, J. *Advanced Organic Chemistry: Reactions, Mechanims, and Structure*, 3rd ed.; Wiley: New York, 1985.
(41) Atkins, P.; de Paula, J. *Physical Chemistry*, 7th ed.; W.H. Freeman: New York, 2001.
(42) Wong, C.-L.; Soriano, A. N.; Li, M.-H. *Fluid Phase Equilib*. **2008**, *271*, 43–52.
(43) Bordi, F.; Colby, R. H.; Cametti, C.; De Lorenzo, L.; Gili, T. *J. Phys. Chem. B* **2002**, *106*, 6887–6893.
(44) Truzzolillo, D.; Bordi, F.; Cametti, C.; Sennato, S. *Phys. Rev. E* **2009**, *79*, 011804−1–011804−3.
(45) Lungwitz, R.; Strehmel, V.; Spange, S. *New J. Chem*. **2010**, in press.